*Supporting Information*

# Compartmentalized Structure Reconstruction in Metal-Organic Frameworks (MOFs) for Efficient Oxygen Evolution Reaction

Lin Ye,[b] Dengrong Sun*[a]

[a] *College of Carbon Neutrality Future Technology, Sichuan University, Chengdu, P. R. China.*

[b] *College of Chemistry, Sichuan University, Chengdu, P. R. China*

E-mail: dengrongsun@hotmail.com; dengrongsun@scu.edu.cn

## Experimental section

**Materials.** All chemicals were obtained from commercial sources and used without further purification. Nickel(II) nitrate hexahydrate ($Ni(NO_3)_2 \cdot 6H_2O$), iron(III) chloride hexahydrate ($FeCl_3 \cdot 6H_2O$), potassium hydroxide (KOH), 1,4-Benzenedicarboxylic acid ($H_2BDC$, B), 2-Aminobenzene-1,4-dicarboxylic acid (ATA, A), Hydrochloric acid (HCl), N, N-dimethylformamide (DMF), Triethylamine (TEA) and ethanol were purchased from Sigma Aldrich Co.

**Synthesis of Ni-BA$_x$.** Ni-BA$_x$ was prepared according to the previously reported procedures with slight modifications.[1] Firstly, 32 mL DMF, 2 mL ethanol and 2 mL ultrapure water were mixed in a 100 mL glass bottle. Then, 0.75 mmol BDC and a certain amount of ATA were added to the above solution and dissolved under ultrasonication. Subsequently, 0.75 mmol $NiCl_2 \cdot 6H_2O$ was added. After $Ni^{2+}$ salts were fully dissolved, 0.8 mL TEA was rapidly injected into the solution. The solution was then stirred for 5 min to obtain a uniform colloidal suspension. Afterwards, the solution was ultrasonicated continuously for 8 h (40 kHz) under confine condition. Eventually, the light green precipitate was collected via centrifugation and washed with ethanol and deionized water, respectively, followed by vacuum freeze-drying for over 12 h to obtain the final product. For comparison, Ni-MOF-B was also synthesized by a similar reaction in absence of ATA.

**Synthesis of Ni-BA$_x$-T.** The Ni-BA$_x$ was placed into a porcelain boat, which was put in the middle of a quartz tube in a furnace under Ar flow. The tube was purged with Ar for 1h before heating to remove oxygen inside. The sample was heated up at a rate of 5 °C/min to 310 °C-330 °C for 1 h, then the furnace was naturally cooled to room temperature to obtain the Ni-BA$_x$-T.

**Synthesis of NiFe-BA$_x$-T.** 15 mg of the as-prepared Ni-BA$_x$-T was dispersed in 10 mL aqueous solution of 5 mM $FeCl_3 \cdot 6H_2O$. The suspension was transferred to a 20 mL glass vial and stirred for 12 h at room temperature. The resulting precipitate was collected by centrifugation at 8000 rpm and washed 3 times with water, followed by vacuum freeze-drying for over 12 h to obtain the NiFe-BA$_x$-T.

## Characterization

The samples were examined by powder X-ray diffraction (PXRD) on a high-resolution powder X-ray diffractometer (DX-2700) with Cu Kα as the radiation source. SEM images were obtained using FIB-SEM (Thermo Scientific Helios 5CX). The 1H NMR were recorded using Bruker AVANCE III Ascend 500 MHz NMR spectrometer. For the 1H NMR analyses, 5 mg of sample was dispersed in 30 μL of HCl. After sonicating for 10 min, 500 μL of DMSO (d6) was added to dissolve the sample. The morphology was studied by field emission transmission electron microscopy (TEM, FEI TECNAI G2 20) and scanning transmission electron microscopy (STEM, FEI TECNAI G2 F20).X-ray photoelectron spectroscopy (XPS) was performed on Thermo Scientific Nexsa, and all binding energies were calibrated by the C 1s peak at 284.8 eV. FT-IR and in-situ FT-IR spectra were scanned with the FT-IR spectrometer (Nicolet iS50FT-IR). The electrochemical measurement was performed using an electrochemical workstation (CHI 760E) with a typical three-electrode system at room temperature.

## Electrochemical measurement

2 mg of sample was dispersed in a mixture of 200 μL $H_2O$, 300 μL ethanol and 20 μL 5wt% Nafion solution. The dispersion was sonicated for 1h to homogeneous disperse the powder. 10 μL of suspension was uniformed loaded on the carbon paper with an area of 0.4*0.5 $cm^2$, which was used as the working electrode. The electrochemical tests were performed in a three-electrode electrochemical cell using a Pt wire and an Hg/HgO electrode as counter electrode and reference electrode, respectively. The oxygen evolution reaction (OER) was performed in the $O_2$-saturated 1 M KOH aqueous solution. The linear sweep voltammetry (LSV) curves were recorded at a rate of 5 mV $s^{-1}$ to minimize capacitive current. All potentials were converted to the reversible hydrogen electrode (RHE) with the following equations: $E_{(RHE)} = E_{(Hg/HgO)} + 0.05916\times pH + 0.098$.

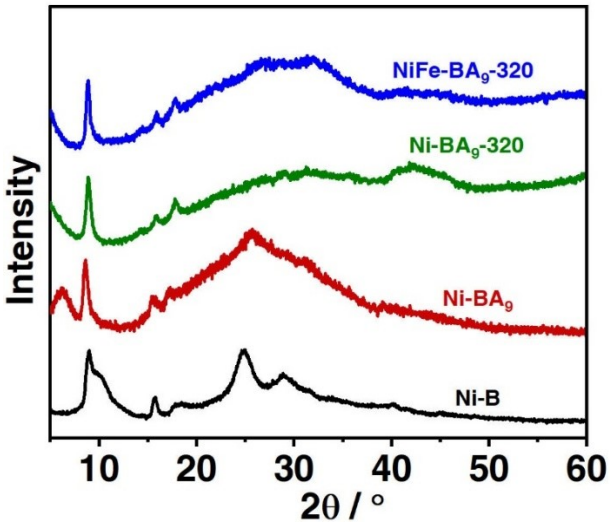


**Fig. S1** XRD diffraction patterns of different samples.

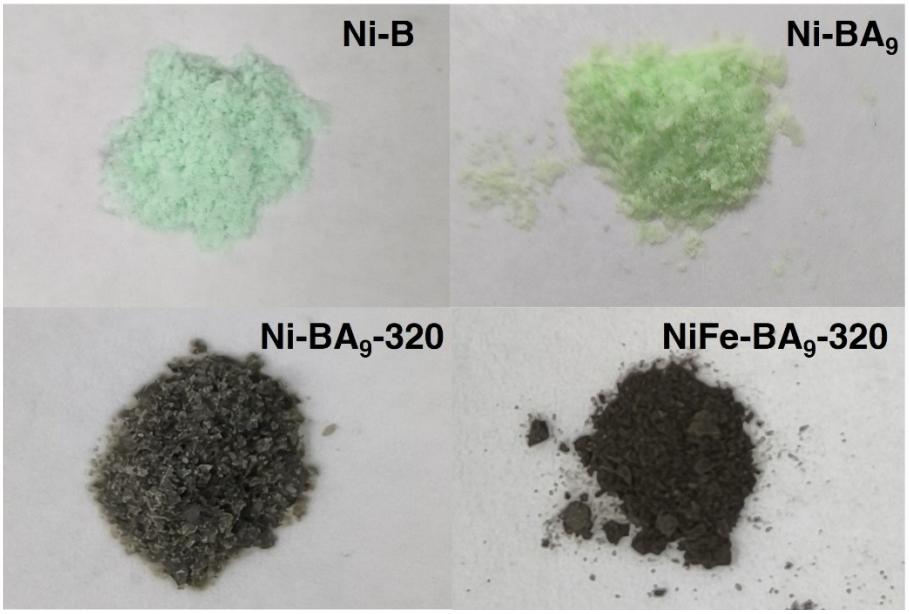


**Fig. S2** The photo images of Ni-B, Ni-$BA_9$, Ni-$BA_9$-320 and NiFe-$BA_9$-320.

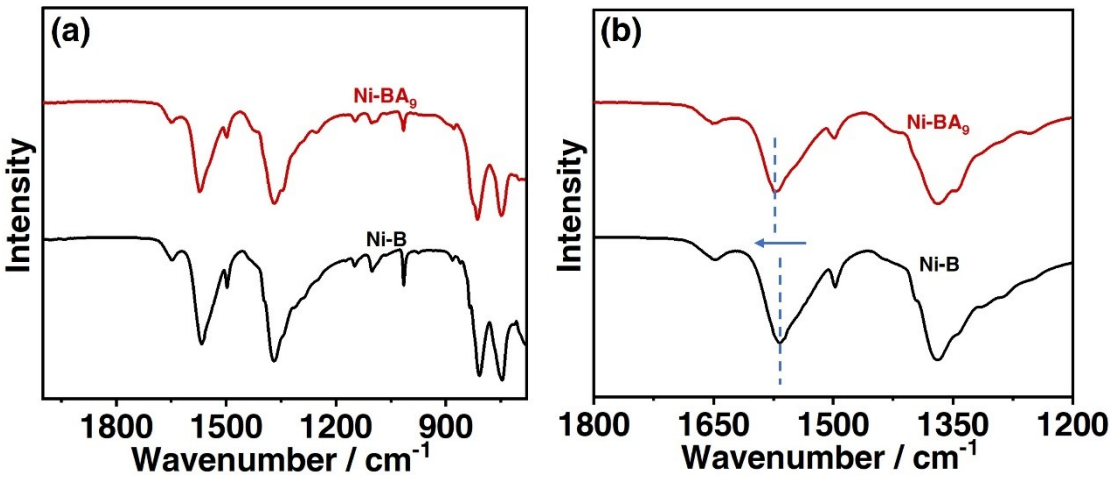


**Fig. S3** The FT-IR spectra of Ni-B and Ni-$BA_9$.

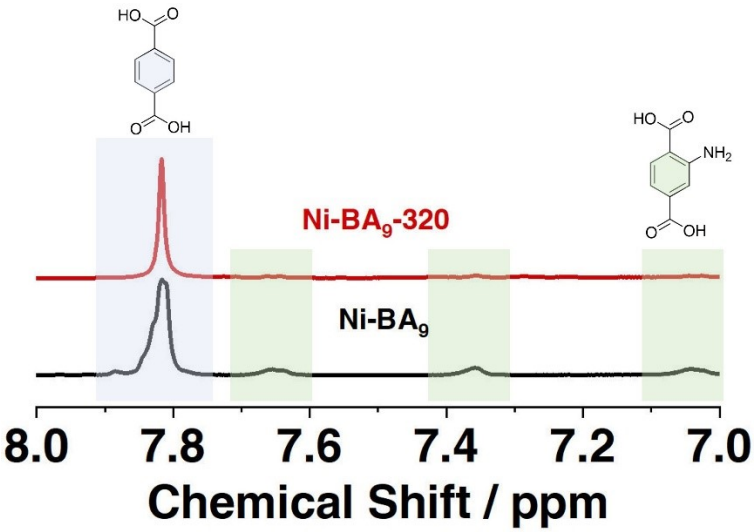


**Fig. S4** The $^{1}$H NMR of Ni-BA$_9$ and Ni-BA$_9$-320.

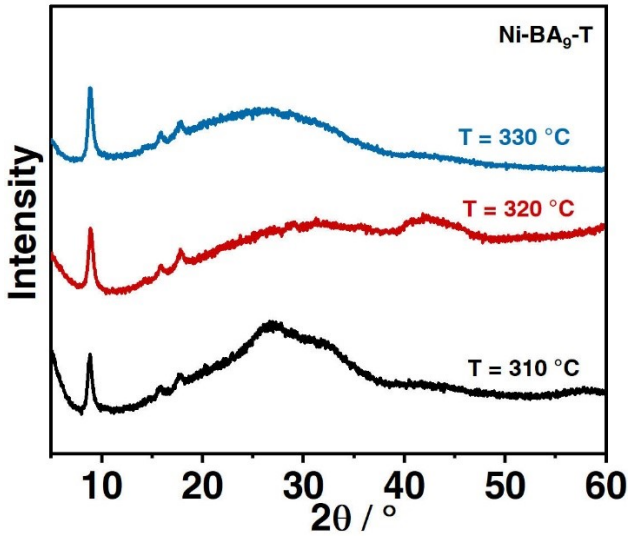


**Fig. S5** XRD diffraction patterns of Ni-$BA_9$-T prepared at different temperature.

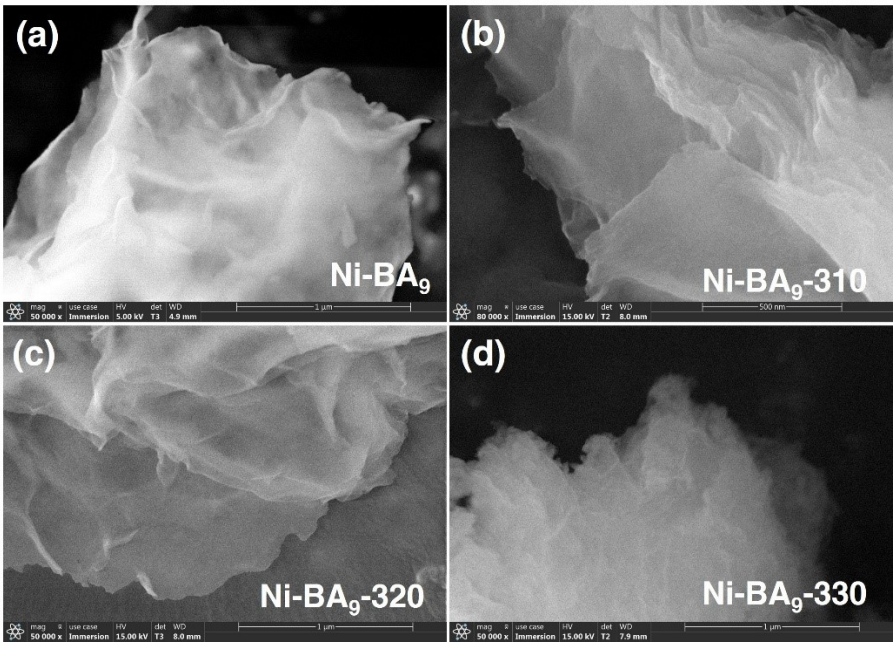


**Fig. S6** SEM images of Ni-$BA_9$ after treating at temperatures ranging from 310°C to 330 °C.

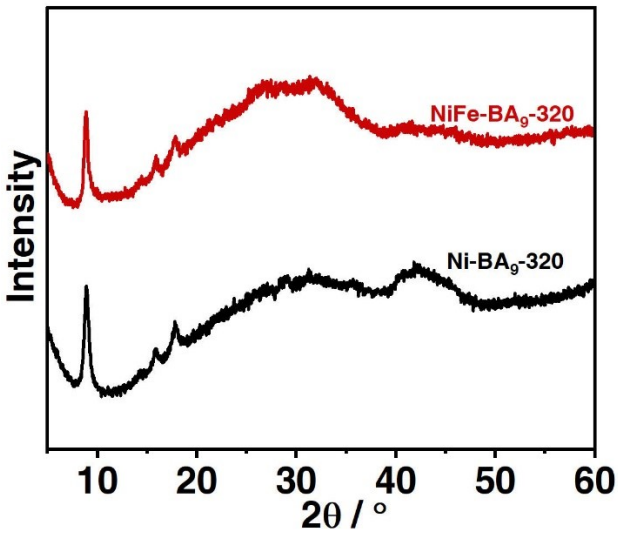


**Fig. S7** XRD diffraction patterns of Ni-$BA_9$-320 and NiFe-$BA_9$-320.

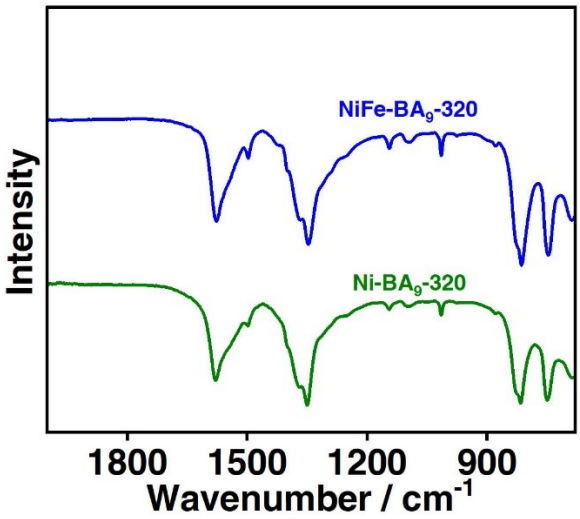


**Fig. S8** Comparison of the FT-IR spectra between Ni-$BA_9$-320 and NiFe-$BA_9$-320.

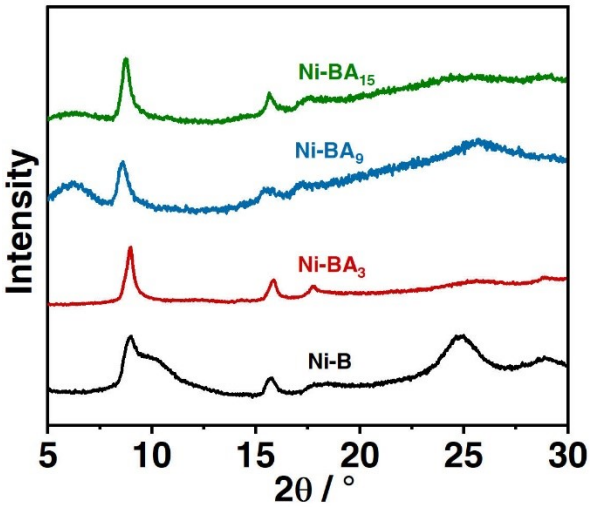


**Fig. S9** XRD diffraction patterns of Ni-$BA_x$ with different amounts of ATA.

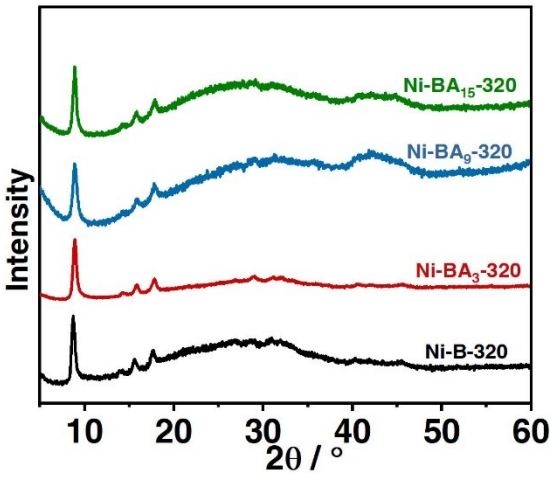


**Fig. S10** XRD patterns of Ni-$BA_x$ with different amounts of ATA prepared at 320 °C.

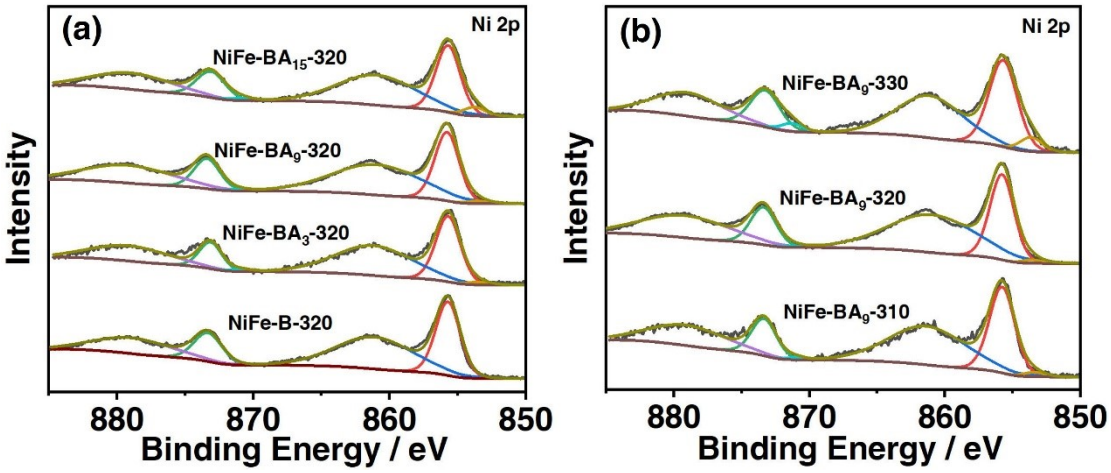


**Fig. S11** XPS spectra in the region of Ni 2p for (a) NiFe-$BA_x$-320; and (b) NiFe-$BA_x$-t prepared at different temperature.

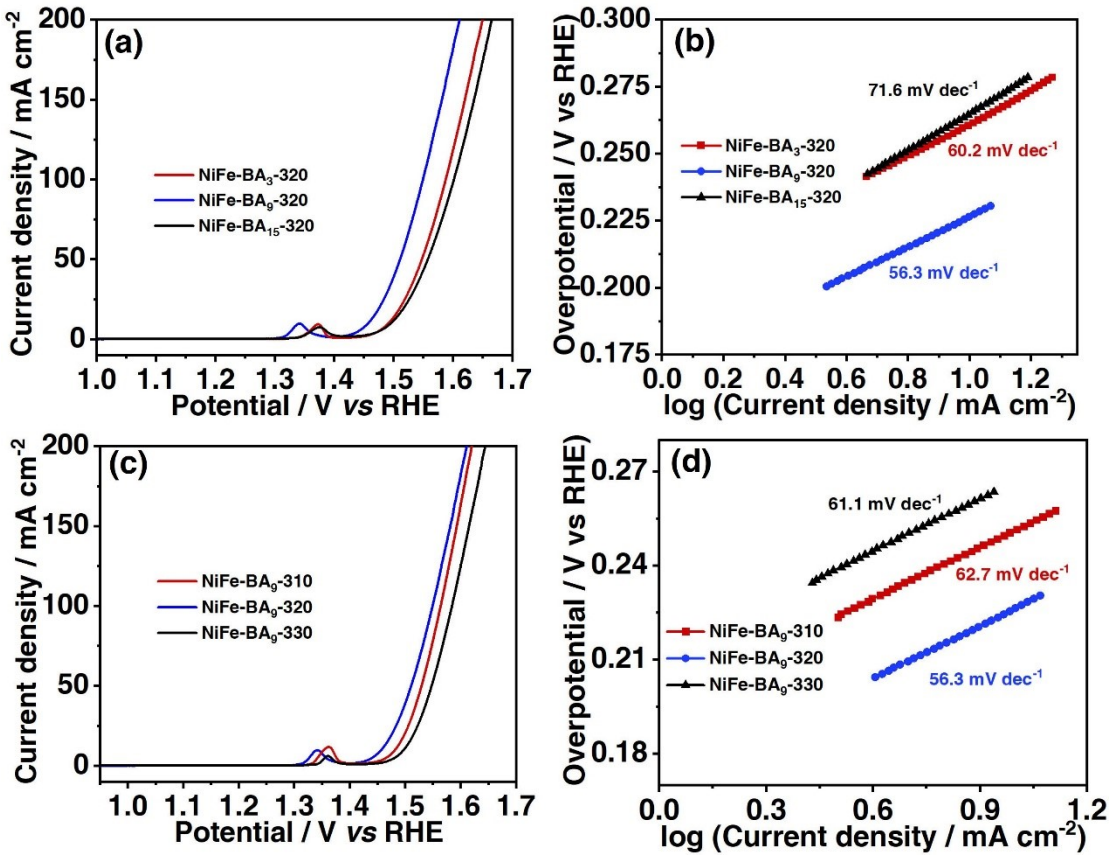


**Fig. S12** (a) LSV and (b)Tafel curves of NiFe-$BA_x$-320; (c)LSV and (d)Tafel curves of NiFe-$BA_9$-T.

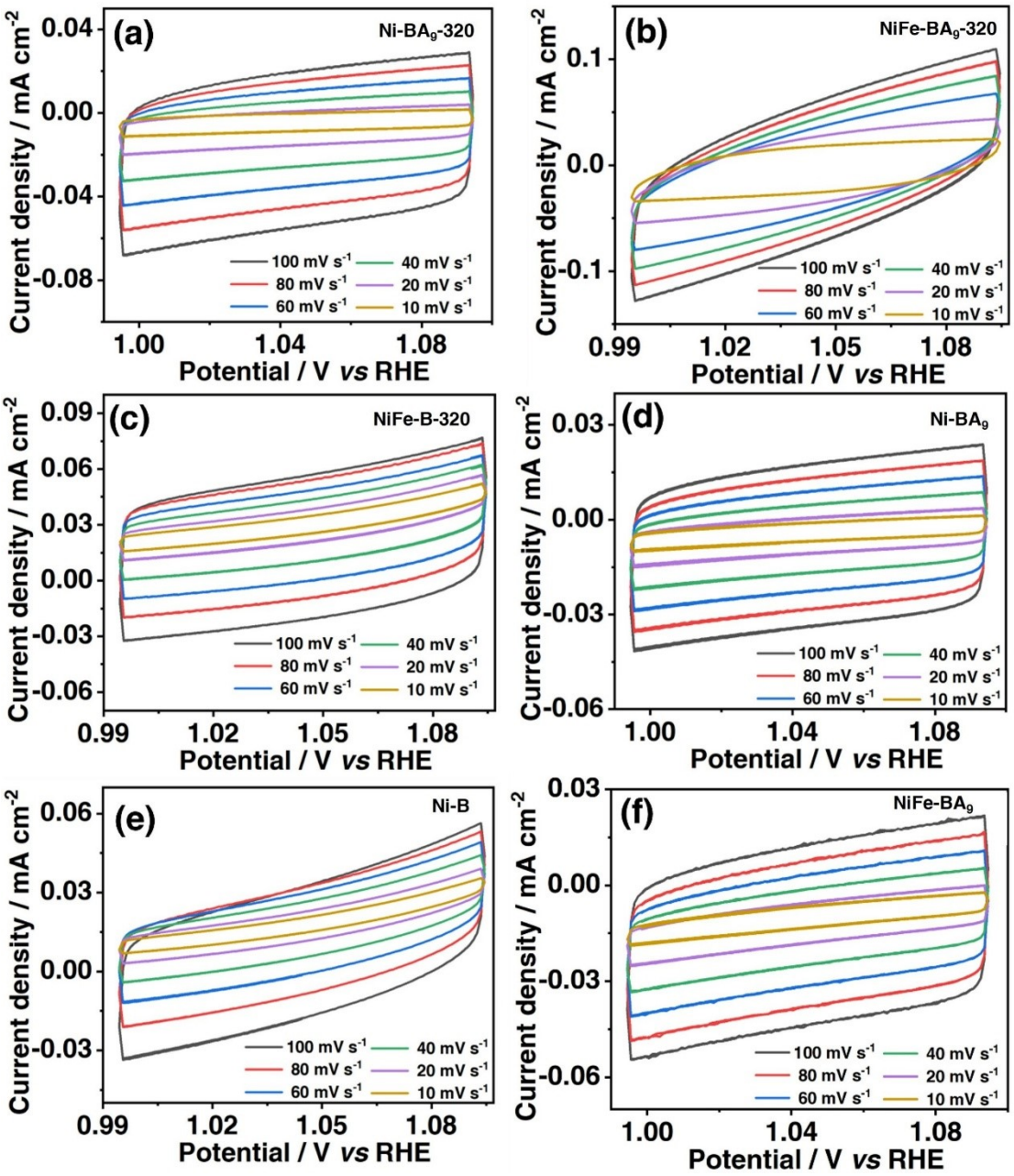


**Fig. S13** CV curves of a series samples at different scan rates.

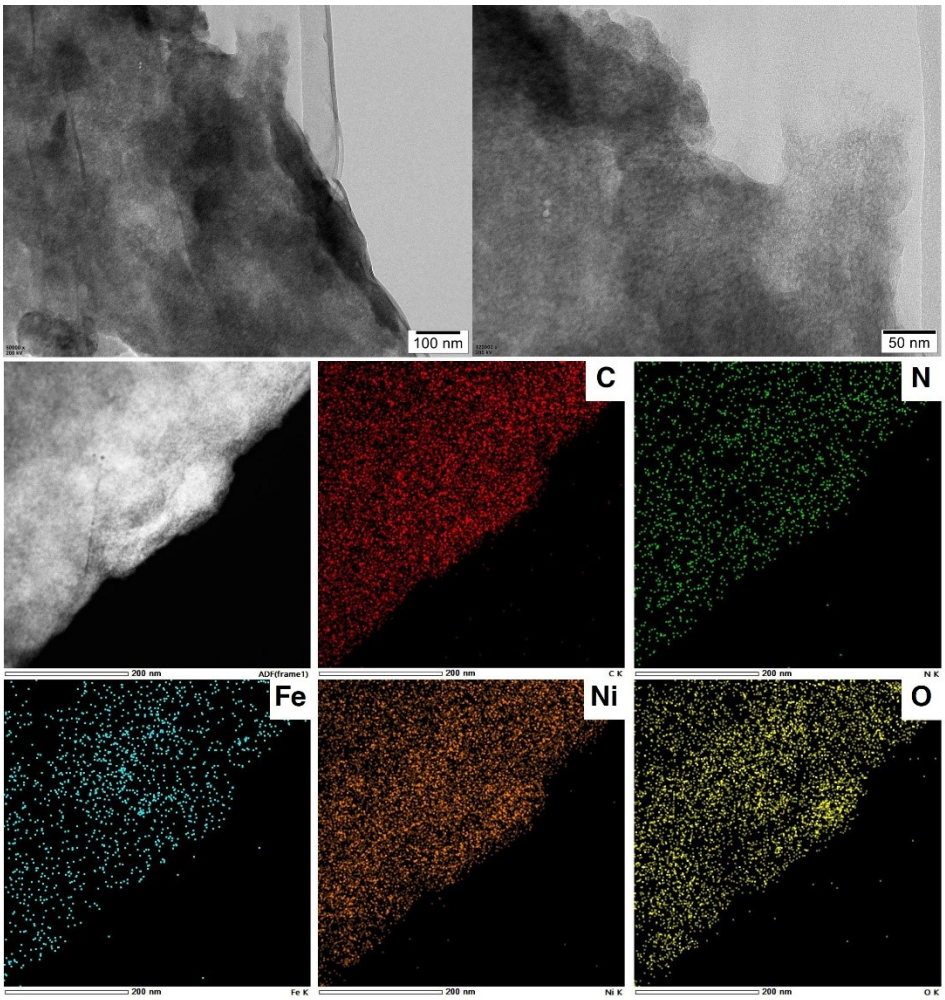


**Fig. S14** TEM and EDS mapping images of NiFe-$BA_9$-320 after OER.

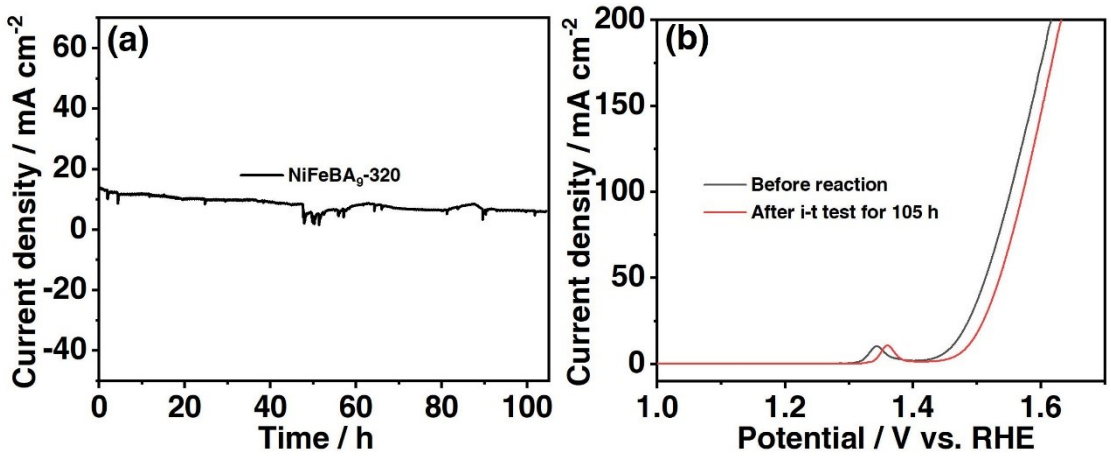


**Fig. S15** (a) Chronoamperometric curves of NiFe-$BA_9$-320 in 1.0 M KOH for 105 h; (b) LSV curves of NiFe-$BA_9$-320 before and after chronoamperometric test.

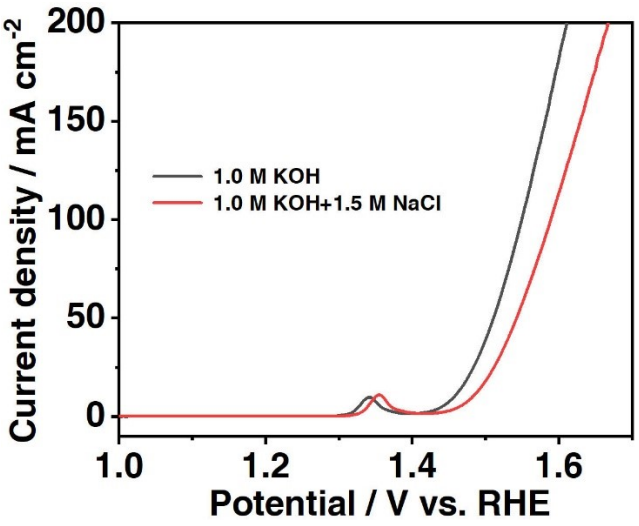


**Fig. S16** LSV curves of NiFe-$BA_9$-320 in 1.0 M KOH and 1.0 M KOH+ 1.5 M NaCl.

**Table S1** Comparison of the OER performance of as-obtained NiFe-$BA_9$-320 with previously reported MOFs-based electrocatalysts.

| Electrocatalyst | Overpotential / mV at 10 mA $cm^{-2}$ | Electrolyte (KOH) | Substrate | Reference |
|---|---|---|---|---|
| **NiFe-$BA_9$-320** | **227** | **1 M KOH** | **CP** | **This work** |
| Ni@CoO@Co-MOF | 247 | 1 M KOH | NF | 1 |
| $Ni_2Fe_1S_q$-zbr-MOFs | 230 | 1 M KOH | CP | 2 |
| Fe/Ni-MOF | 188 | 1 M KOH | NF | 3 |
| NiBDC-FcCA/Fe foam | 206 | 1 M KOH | Fe foam | 4 |
| Ni(DMBD)-MOF/NF | 295 | 1 M KOH | NF | 5 |
| $Ni_{0.5}Co_{0.5}$-MOF-74 | 270 | 1 M KOH | GC | 6 |
| $(Ni_2Co_1)_{0.925}Fe_{0.075}$-MOF-NF | 257 | 1 M KOH | NF | 7 |
| $NiFe_2O_4$/NiFe LDH@Ni-BDC | 251 | 0.85 M KOH | CP | 8 |
| $Fe_{10}$Ni-$BA_{7.0}$-T | 286 | 1 M KOH | CP | 9 |
| Br-Ni-MOF(A) | 306 | 1 M KOH | CP | 10 |
| CoCu-MOF NBs | 271 | 1 M KOH | CP | 11 |
| IrNi@NiFe-MOFs | 229 | 1 M KOH | GC | 12 |
| NiFe-THQ | 272 | 1 M KOH | GC | 13 |
| CoNiMOF-mCNTs | 306 | 1 M KOH | GC | 14 |
| CoFe-MOF-74 | 280 | 1 M KOH | GC | 15 |
| $CoNi_2$-MOF | 240 | 0.1 M KOH | GC | 16 |
| HE(Ru,Mo)-MOFs | 267 | 1 M KOH | GC | 17 |
| NiFe MOF | 221 | 1 M KOH | NF | 18 |
| NiFc-MOF | 270 | 1 M KOH | Graphite | 19 |
| (Fe,Ni)OOH-MOF/NF | 229 | 1 M KOH | NF | 20 |

GC: glass carbon electrode, NF: Nickel foam, CP: carbon paper

**References**


1. Y. R. Wang, A. Wang, Z. Z. Xue, L. Wang, X. Y. Li and G. M. Wang, *J. Mater. Chem. A* 2021, **9**, 22597.

2. S. Kandambeth, V. S. Kale, D. Fan, J. A. Bau, P.M. Bhatt, S. Zhou, A. Shkurenko, M. Rueping, G. Maurin, O. Shekhah and M. Eddaoudi, *Adv. Energy Mater.* 2022, **13**, 2202964.

3. D. Ye, L. H. Fu, Y. Tang, D. Zhang and T. Liu, *J. Mater. Chem. A*, 2025, **13**, 12057.

4. Y. Q. Zhang, M. Liu, L. T. Zhang, N. Lu, X. M. Wang, Z. G. Li, X. H. Zhang, N. Li, X. H. Bu, *Adv. Funct. Mater.* 2025, **35**, 2412406.

5. Y. Z. Liu, X. T. Li, S. F. Zhang, Z. L. Wang, Q. Wang, Y. H. He, W. H. Huang, Q. D. Sun, X. Y. Zhong, J. Hu, X. Y. Guo, Q. Lin, Z. Li, Y. Zhu, C. C. Chueh, C. L. Chen, Z. T. Xu and Z. L. Zhu, *Adv. Mater.* 2023, **35**, 2300945

6. S. L. Zhao, C. H. Tan, C. T. He, P. F. An, F. Xie, S. Jiang, Y. F. Zhu, K. H. Wu, B. W. Zhang, H. J. Li, J. Zhang, Y. Chen, S. Q. Liu, J. C. Dong and Z. Y. Tang, *Nat. Energy* 2020, **5**, 881.

7. Q. Z. Qian, Y. P. Li, Y. Liu, L. Yu, G. Q. Zhang, *Adv. Mater.* 2019, **31**, 1901139.

8. R. Y. Hou, X. X. Yang, L. H. Su, W. L. Cen, L. Ye and D. Sun, *Nanoscale* 2023,**15**, 18858-18863.

9. D. Sun, L.W. Wong, H. Y. Wong, K. H. Lai, L. Ye, X. Y. Xv, T. H. Ly, Q. M. Deng and J. Zhao, *Angew. Chem. Int. Ed.* 2023, **62**, e202216008.

10. W. R. Cheng, S. B. Xi, Z. P. Wu, D. Y. Luan and X. W. Lou, *Sci. Adv.* 2021, **7**, eabk0919.

11. W. C. Cheng, Z. P. Wu, D. Y. Luan, S. Q. Zang and X. W. Lou, *Angew. Chem. Int. Ed.* 2021, **60**, 26397

12. J. Z. Jia, Y. T. Wang, Y. Y. Cha, Z. W. Wang, J. F. Huang, D. N. Wang, H. Li, K. L. Guo, J. Li, J. E. Huang, Y. Tang and C. L. Xu, *Adv. Funct. Mater.* 2025, 2500568

13. L. Zhao, J. Yan, H. Huang, X. Du, H. Chen, X. He, W. Li, W. Fang, D. Wang, X. Zeng, J. Dong and Y. Liu, *Adv. Funct. Mater.* 2024, **34**, 2310902.

14. S. Yu, Y. Wu, Q. Xue, J. J. Zhu and Y. Z. Zhou, *J. Mater. Chem. A* 2022, **10**, 4936-

4943

15. X. Zhao, B. Pattengale, D. Fan, Z. Zou, Y. Zhao, J. Du, J. Huang and C. Xu, *ACS Energy Lett.* 2018, **3**, 2520.
16. W. Zhou, D. D. Huang, Y. P. Wu, J. Zhao, T. Wu, J. Zhang, D. S. Li, C. H. Sun, P. Y. Feng and X. H. Bu, *Angew. Chem. Int. Ed.* 2019, **58**, 4227.
17. X. Q. Mu, M. Yu, X. Y. Liu, Y. R. Liao, F. J. Chen, H. Z. Pan, Z. Y. Chen, S. L. Liu, D. S. Wang and S. C. Mu, *ACS Energy Lett.* 2024, **9**, 5763-5770.
18. Y. Liu, X. Li, Q. Sun, Z. Wang, W.-H. Huang, X. Guo, Z. Fan, R. Ye, Y. Zhu, C.-C. Chueh, C.-L. Chen and Z. Zhu, *Small* 2022, **18**, 2201076.
19. J. Hu, Q. Xu, X. Wang, X. Huang, C. Zhou, Y. Ye, L. Zhang, H. Pang, *Carbon Energy* 2023, **5**, e315.
20. Y. B. Huang, H. J. Xie, Z. L. Gu, A. Q. Kong, J. W. Wang, W. Guo, H. T. Zhang, J. C. Liu, C. H. Sun and F. X. Bao, *App. Catal. B: Environ.* 2025, **371**, 125221.